RSC Advances

ROYAL SOCIETY
OF CHEMISTRY

www.rsc.org/advances

The hydrolysis mechanism of polyglycolic acid under the tensile mechanical loading: a density functional theory study

Shin-Pon Ju[1,2]**, Wei-Chun Huang*[1]*, Chien-Chia Chen*[1]

[1]*Department of Mechanical and Electro-Mechanical Engineering, National Sun Yat-Sen University, Kaohsiung, Taiwan 804*

[2]*Department of Medicinal and Applied Chemistry, Kaohsiung Medical University, Kaohsiung, Taiwan 807*

ABSTRACT

The hydrolysis mechanisms of polyglycolic acid (PGA) under tensile mechanical loading were studied by the density functional theory (DFT) calculation for illustrating the enhancement of PGA hydrolysis by external mechanical loading founded in previous experimental studies (Iranian Polymer Journal **17** (9), 691-701 (2008)). Before the hydrolysis degradation begins, PGA firstly forms the PGA hydrolysis intermediate by combining one water molecule at the carbonyl carbon and then the C-O alkyl bond is ruptured after the hydrogen atom transfers from the carbonyl oxygen to the alkyl oxygen. Consequently, the effects of tensile forces imposed on the PGA and PGA intermediate were both studies. The variations of bending angle, torsion angle, and bond length as well as the electronic properties of PGA and its intermediate at different strains were presented. From the force-strain profiles of PGA and PGA intermediate, it reveals the tensile force on the PGA can be relaxed once the PGA forms the PGA intermediate, leading to the stabilization of PGA material under external mechanical loading. After the calculation of the nudge-elastic band (NEB) method, the results reveal that the energy barrier for the dissociation of the PGA intermediate into two PGA molecules significantly decreases under the increasing force, which induces the PGA hydrolysis. Our DFT calculation results have provided a clear explanation for the experimental observation, where the mechanical loading enhances the PGA degradation rate.

KEYWORDS: polyglycolic acid, density functional theory, hydrolysis mechanism, electronic properties.

AUTHOR INFORMATION

Corresponding Author*

E-mail: jushin-pon@mail.nsysu.edu.tw Fax: 886-7- 5252132

Tel: 886-7-5252000 Ext. 4231

I. Introduction

Polyglycolic acid (PGA) is one of the synthetic polymers with biologically decomposable characteristics and has therefore been extensively used in physical and cosmetic surgery for surgical sutures [1], vascular stents [2], and cartilage support [3]. The decomposition of PGA can be mainly attributed to the hydrolysis effect; during the decomposition process the PGA main chain is disconnected, and its molecular weight decreases.

It has been proven that the mechanical loading on PGA material has a significant effect on its degradation rate [4]. Since PGA and PGA composite materials can be used as a temporary bone bracket [5], the internal stress coming from the relative movement between the bone and PGA material influences the PGA degradation rate. Consequently, understanding the influence of stress on the PGA material is very important to further expand the applications of similar biodegradable polymers.

In previous experimental and theoretical studies, the force imposed on molecules could be regarded as a catalyst to lower the energy barrier necessary for decomposition. For example, Wiita applied mechanical force to a disulphide bond substrate by single-molecule force-clamp spectroscopy and monitored the reduction of these bonds by individual enzymes [6]. Their results show that a mechanical force can significantly alter the chemistry of the catalytic site in thioredoxin. Li's study elucidated the effect of force imposed on the reaction center for disulfide bond reduction by combining transition path sampling and quantum/classical mechanical simulations. Their results show that force can significantly increase the reaction rate and reduce the distance required for conversion to the required transition state [7]. Ainavarapu used both experiments for single-molecule as well as high-level quantum chemical calculations to probe the transition state of disulfide bond reduction for a bimolecular nucleophilic substitution (S_N2)

reaction. They obtained the force-dependent rate constants of the disulfide bond reduction. Their studies have proved that an atomic force can significantly improve the reaction rate and reduce the reaction barrier [8]. In a theoretical study, Röhrig conducted the first-principles simulations of cis-polyacetylene fragments under tensile stress. By applying the tensile stress, the energy barrier of a cis-trans isomerization of conjugated carbon–carbon double bonds is lowered by 5 or possibly even 10 kcal/mol [9]. In Beryer's study [10], the length r of the rupture bond was elongated from its equilibrium length by sequential elongation steps, after which the full geometry optimization was carried out at the fixed r. Then the forces imposed on the atoms connected by the fixed bond were determined. This method is also named "COnstrained Geometries simulate External Force'' (COGEF) method. Ribas-Arino *et al.* modified COGEF by explicitly including the forces imposed on two atoms connected by the bond they concerned [11]. They called this method as "External Force is Explicitly Included" (EFEI) method by which the forces can reflect the realistic situation in the force-clamp AFM experiments. By ab initio calculation, Dopieralski *et al.* investigated the mechanically assisted ring-opening reactions of the gem-dichlorocyclopropane (gDCC) systems for understanding the force-dependence of activation energies [12]. From the predicted selectivity, it was found that the ring-opening of cis gDCC is higher than the trans isomers. Accordingly, under stress conditions the cis gDCCs were found to react much faster than the trans isomers. In their further study [13], ab initio simulations were further used to find a dual role of the mechanical force for the cleavage of a protein disulfide bond through the reaction with hydroxide ions. From their simulation results, they proposed that the external force imposed on the system can accelerate the reaction as well as cause a conformational distortion of the S–S–C–C dihedral angle. This distorted conformation is shielded against nucleophilic attack, which reduces the acceleration of the reaction rate of a protein disulfide bond. Their findings from ab initio calculation clearly explained the experimental observation, which the acceleration of the reaction rate is substantially reduced for a protein disulfide bond as the imposed force exceeds 0.5 nN.

To the best of our knowledge, there have been no studies on the hydrolysis mechanism for PGA material under mechanical loading using the theoretical approach. Therefore, the density functional theory calculation was used here to investigate the electronic properties of PGA and the PGA intermediate at different mechanical loading. The force-dependent energy barrier for the hydrolysis was also presented.

II. Simulation model

DFT calculations implemented by the Dmol3 package [14, 15] were adopted to study the relationship between the strain and the tensile force as well as the corresponding electronic properties of PGA. All electron calculations were employed with double numerical basis sets plus d-functions (DND) and the generalized gradient approximation (GGA) [16]with the Becke-Lee-Yang-Parr (BLYP) generalized gradient approximation correction [17]. Mulliken population analysis was used to obtain the charge on each atom at different strains. For the tensile simulation of the infinite PGA chain, a PGA model with 3 monomers was placed in a periodic boundary box in the x-, y-, and z-dimensions. The backbone of the PGA is along the z dimension shown in Fig. 1, with the x and y box lengths long enough to prevent PGA from interacting with its PBC image. The PGA was first optimized by adjusting the z-dimensional length of the box until the force in the z direction is close to zero. After the optimization process, the initial box size was $10\times10\times10.5(\text{Å}^3)$ before the tensile simulation. The tensile strain was implemented by increasing the length of the z dimension with the increment of 0.013 Å. The PGA was then completely optimized before the application of the next increment in the z dimension. The strain ε in the stress direction was calculated by the following equation:

$$\varepsilon = \frac{l_{z(t)} - l_{z(0)}}{l_{z(0)}} \quad (1)$$

where $l_{z(t)}$ is the z-dimensional length of the simulation box after implementing t times of elongation increments, and $l_{z(0)}$ is the initial length of the simulation box in the z direction. Consequently, the strain is a parameter with the dimensionless unit.

III. Result and Discussion

Because the hydrolysis occurs near the acyl carbon (C_1 in Fig. 1) of the ester, the variations of bending angles at O_1-C_1-C_2 and torsion angles of C_3-O_1-C_1-C_2 with increasing strain were investigated. Fig. 2 shows the relationship of the tensile force with the strain and the variations of bending and torsion angles for a PGA chain under tension. The required energy to change the torsion angle is lower than that to change the beading angle, so the variation of torsion energy is more significant than the bending angle in order to relax the PGA structure under the external tensile loading. At strains smaller than 0.035, the force increases linearly with the strain and the bending angle only increases slightly with increasing strain. The torsion angle increases more significantly with the increasing strain, revealing that PGA configuration is distorted under the small tensile strain. From strains of 0.035 to 0.1, the slope of the force-strain curve becomes slightly larger than that at the strains below 0.035, and the changes of both bending and torsion angles significantly increase with increasing strain. The slope of the torsion angle variation with strain is smaller than those during strains from 0 to 0.035 because the bending angle change also participates in the structural relaxation. As strain becomes higher than 0.1, the torsion angle shows a slight increase with little variation, and approaches its maximal value. The inset of Fig.2

shows the total energy variation of PGA with the tensile strain. Two dashed lines at strains of 0.035 and 0.1 are used to indicate the energy variation at these two strains. The total energy undergoes only a small increase as the strain rises from 0 to 0.035 with total energy increasing more significantly with strains from 0.035 to 0.1. As the strain becomes larger than 0.1, the increase of total energy is proportional to the increase of strain.

Fig. 3 displays the bond length variations of C_1-O_1, C_1-C_2, and C_1-O_2 pairs with the strain. The values in the parentheses are the corresponding bond lengths of these pairs at a strain of 0. The C_1-O_2 bond is normal to the tensile direction and becomes only slightly shorter by 0.009Å, a decrease of 0.74%, as the strain increases to 0.15. For C_1-O_1 and C_1-C_2 bonds at strains less than 0.035, they are forced to align along the tensile direction when the strain increases because the bending angle gradually becomes larger. The lengths of C_1-O_1 and C_1-C_2 bonds increase by 0.016 Å at strain of 0.035, increases of about 1.15% and 1.04% from their lengths at strain of 0. When the strain increases from 0.035 to 0.15, the magnitudes of the elongations of C_1-O_1 and C_1-C_2 bonds are about 6.07% and 9.8% longer than those at strain of 0, indicating the length of C_1-C_2 bond is relatively sensitive to the strain.

The Mulliken charge variations of alkyl oxygen (O_1), carbonyl oxygen (O_2), carbonyl carbon (C_1), and C_2 atoms are shown in Fig. 4, with the values shown in parentheses indicating the Mulliken charges of the corresponding atoms at strain of 0. At strain of 0, the charges of C_1 and C_2 atoms are 0.588e and -0.116e, and the charges of O_1 and O_2 atoms are -0.469e and -0.405e, respectively. As the strain gradually increases from 0 to 0.15, the Mulliken charge variations of C_1 and O_1 atoms become more negative while those of C_2 and O_2 atoms become more positive, indicating more electrons transfer from C_2 and O_2 atoms to C_1 and O_1 atoms at higher strains.

Fig. 5 shows the force-strain profile for the PGA hydrolysis intermediate at different strains. The intermediate structure can be seen in the upper right panel of Fig. 5, a structure coming from the combination of PGA and a water molecule as shown in the bottom right panel of Fig.5. For comparison, the PGA force-strain profile is also shown in Fig. 5. At strain of 0.1, the tensile force exerted on the PGA is about 3.56 nN. For comparison of the tensile force relaxation after the PGA becomes the PGA intermediate, the initial structure of the PGA intermediate derives from the PGA structure at strain of 0.1, and H1 and O3 H2 were added to O2 and C1 atoms to form PGA intermediate. Consequently, the force-strain profile of the PGA intermediate begins from strain of 0.1. After the geometric optimization of the PGA intermediate, the tensile force originally imposed on PGA is relaxed to a much lower value of 0.45 nN. This implies that mechanical force on PGA can be relaxed once the PGA intermediate appears, helping to stabilize the PGA material under the mechanical loading. The profile of energy variation with the strain for the PGA intermediate is shown in the lower right inset of Fig. 5, indicating that the energy slightly increases with the strain lower than 0.2 and monotonically increases with the strain larger than 0.2.

Fig. 6 shows the profiles of bond length variations with the strain for C_1-C_2, C_1-O_1, C_1-O_2, and C_1-O_3 bonds for the PGA intermediate. The values in the parentheses are the bond lengths of the corresponding pairs at strain of 0.11. The variations of C_1-O_2 and C_1-O_3 are comparatively not sensitive to the strain, with C_1-C_2 and C_1-O_1 clearly increasing with increasing strain. The corresponding Mulliken charge variations are presented in Fig. 7, which shows the profiles of charge variations with strain for C_1, C_2, O_1, O_2, and O_3 atoms. Mulliken charges of these atoms at strain of 0.1 are shown in parentheses. The charges of O_2 and O_3 atoms become more positive with increasing strain, whereas the charges of C_1, C_2, and O_1 become more negative. It should be noted the charge of C_2 atoms of the PGA intermediate becomes more negative, but, for PGA, the charge of C_2 atoms becomes more positive when the strain increases.

The hydrolysis of polyester is a bimolecular nucleophilic substitution reaction (S_N2), and one water molecule is first added at the carbonyl carbon to form the ester hydrolysis intermediate. Then the C-O alkyl bond is ruptured after the hydrogen atom transfers from the carbonyl oxygen to the alkyl oxygen [18]. Previous ab initio study also used this mechanism to study the C-O cleavage process for the hydrolysis of ethyl acetate [19]. The similar reactant and product was used to search the minimal energy pathway (MEP) for the C-O cleavage during the PGA hydrolysis. Moreover, the first stage of polyester hydrolysis is the saturation of water during which the diffusion of water into the polymer takes place [18, 20]. With the increasing water content within the amorphous polyester, the degradation rate increases. Since the PGA hydrolysis happens at a low water weight fraction instead of an aqueous solution, the solvation model was not included in the current DFT calculation. Fig. 8 depicts the MEP for PGA hydrolysis, where the H_1 atom transfers to the O_1 atom to form the OH group and then the O_2 atom bonds with the C_1 atom by a double bond, resulting in the dissociation of PGA chains as shown in the rightmost structure in Fig. 8. Note that here a molecule of PGA intermediate was used for the simulation, different from the PBC model shown in Figs. 1 and 5, because the PGA PBC model will be only a single PGA molecule after the breakage of the C_1-O_1 bond due to the H_1 atom transferring from O_2 to O_1. The current model is very similar to those used in previous studies about the force catalyst effect [6]. The PGA intermediate and the two PGA molecules resulting from the dissociation of the PGA intermediate were first optimized. Then the nudge-elastic band (NEB) method was used to find the transition state connecting these two configurations. The energy barrier for the hydrolysis of PGA intermediate is about 32.2 kcal/mol.

Fig. 9 shows the energy barriers at different tensile forces on the PGA intermediate. The distance between the two end oxygen atoms is about 6.093 Å for the fully optimized PGA intermediate, so this distance is used as the reference length for the strain of 0. This distance was increased to represent PGA intermediate under different strains and the NEB was used after each strained PGA intermediate had completed optimization. It is apparent that the stressed PGA intermediate configuration can decrease the energy barrier for the hydrolysis process. In Fig. 7, the O_2 atom becomes less negative with increasing strain, implying that the OH bond strength is weakened by the strain. On the other hand, the O_1 atom becomes more negative when the strain increases. This situation is very beneficial for attracting the H_1 atom and lowers the H_1 energy barrier, allowing for a bond change from the O_2 to the O_1 atom to enhance the occurrence of PGA hydrolysis.

III. Conclusion

The density functional theory calculation has been used to study the biodegradation mechanisms of hydrolysis under the tensile force stress for polyglycolic acid (PGA). The results show the bending angles and torsion angels of PGA increase with the increasing strain, and the tensile force also linear increases with the strain. As the strain gradually increases from 0 to 0.15, the Mulliken charges of C_1 and O_1 atoms become more negative while those of C_2 and O_2 atoms become more positive, indicating more electrons transfer from C_2 and O_2 atoms to C_1 and O_1 atoms at higher strains.

Once the PGA becomes the PGA intermediate by combining with a water, the tensile force of 3.56 nN on PGA at the strain of 0.1 will be relaxed to a lower value of 0.45 nN, which helps the increase of the stability of the PGA material. The Mulliken charges of O_2 and O_3 atoms become more positive with the increasing strain, whereas the charges of C_1, C_2, and O_1 become more negative.

NEB calculation results provide the evidence of the force catalysis effect on the PGA intermediate, which the dissociation barrier is significantly reduced by the tensile force, leading to a significant increase in the PGA intermediate dissociation rate. Our DFT calculation results have provided an analysis procedure to evaluate the dissociation mechanism for other biodegradable materials and whether or not the mechanical loading enhances the degradation rate.

ACKNOWLEDGMENT

The authors would like to thank (1) National Science Council of Taiwan, under Grant No. NSC101-2628-E-110-003-MY3, and (2) National Center for High-performance Computing, Taiwan, for supporting this study.

Figure Caption

Fig. 1 Physical model of polyglycolic acid.

Fig. 2 The force-strain profile with the variations in bending and torsion angles for a PGA chain under tension. The inset presents the variation of energy with strain.

Fig. 3 The bond length variations of C_1-O_1, C_1-C_2, and C_1-O_2 pairs with strain.

Fig. 4 The Mulliken charge variations of O_1, O_2, C_1, and C_2 atoms

Fig. 5 The force-strain profile for the PGA hydrolysis intermediate at different strains. (upper inset) Structure from the combination of PGA and a water molecule; (bottom left inset) PGA intermediate structure; and (bottom right inset) the variation of energy with strain for PGA intermediate.

Fig. 6 Profiles of bond length variations with the strain for C_1-C_2, C_1-O_1, C_1-O_2, and C_1-O_3 bonds.

Fig. 7 Charge variations with strain for C_1, C_2, O_1, O_2, and O_3 atoms.

Fig. 8 Minimal energy pathway (MEP) for PGA intermediate degradation.

Fig. 9 Energy barriers at different tensile force for the PGA intermediate.

REFERENCES

1. D. E. Cutright, J. D. Beasley III and B. Perez, *Oral Surgery, Oral Medicine, Oral Pathology*, 1971, **32**, 165-173.
2. A. M. Reed and D. K. Gilding, *Polymer*, 1981, **22**, 494-498.
3. L. E. Freed, D. A. Grande, Z. Lingbin, J. Emmanual, J. C. Marquis and R. Langer, *Journal of Biomedical Materials Research*, 1994, **28**, 891-899.
4. R. Mohammadikhah and J. Mohammadi-Rovshandeh, *Iranian Polymer Journal*, 2008, **17**, 691-701.
5. N. Dunne, V. Jack, R. O'Hara, D. Farrar and F. Buchanan, *Journal of Materials Science-Materials in Medicine*, 2010, **21**, 2263-2270.
6. A. P. Wiita, R. Perez-Jimenez, K. A. Walther, F. Gräter, B. Berne, A. Holmgren, J. M. Sanchez-Ruiz and J. M. Fernandez, *Nature*, 2007, **450**, 124-127.
7. W. Li and F. Gräter, *Journal of the American Chemical Society*, 2010, **132**, 16790-16795.
8. S. R. Koti Ainavarapu, A. P. Wiita, L. Dougan, E. Uggerud and J. M. Fernandez, *Journal of the American Chemical Society*, 2008, **130**, 6479-6487.
9. U. F. Röhrig and I. Frank, *The Journal of Chemical Physics*, 2001, **115**, 8670.
10. M. K. Beyer, *The Journal of Chemical Physics*, 2000, **112**, 7307-7312.
11. J. Ribas-Arino, M. Shiga and D. Marx, *Angewandte Chemie International Edition*, 2009, **48**, 4190-4193.

12. P. Dopieralski, J. Ribas-Arino and D. Marx, *Angewandte Chemie International Edition*, 2011, **50**, 7105-7108.
13. P. Dopieralski, J. Ribas-Arino, P. Anjukandi, M. Krupicka, J. Kiss and D. Marx, *Nat Chem*, 2013, **5**, 685-691.
14. B. Delley, *The Journal of Chemical Physics*, 1990, **92**, 508-517.
15. B. Delley, *The Journal of Chemical Physics*, 2000, **113**, 7756-7764.
16. J. P. Perdew, K. Burke and M. Ernzerhof, *Physical Review Letters*, 1996, **77**, 3865-3868.
17. P. M. W. Gill, B. G. Johnson, J. A. Pople and M. J. Frisch, *Chem Phys Lett*, 1992, **197**, 499-505.
18. S. Lyu, J. Schley, B. Loy, D. Lind, C. Hobot, R. Sparer and D. Untereker, *Biomacromolecules*, 2007, **8**, 2301-2310.
19. G. Schmeer and P. Sturm, *Phys Chem Chem Phys*, 1999, **1**, 1025-1030.
20. S. Hurrell and R. E. Cameron, *Biomaterials*, 2002, **23**, 2401-2409.

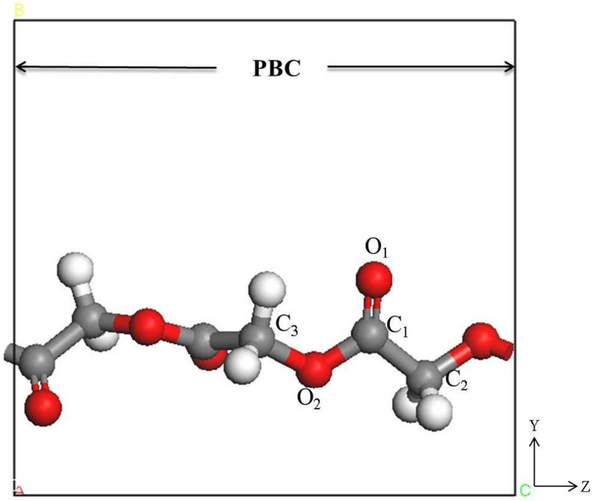

Fig. 1 Physical model of polyglycolic acid.

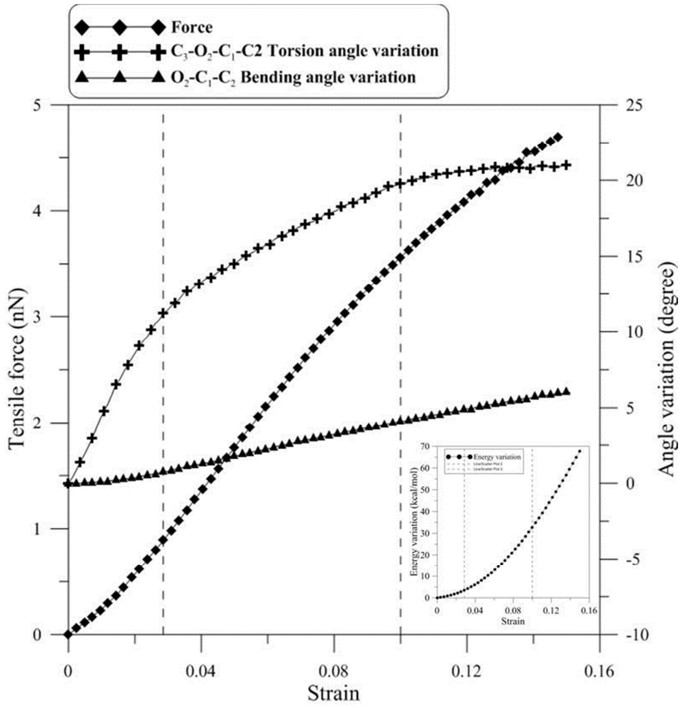

Fig. 2 The force-strain profile with the variations in bending and torsion angles for a PGA chain under tension. The inset presents the variation of energy with strain.

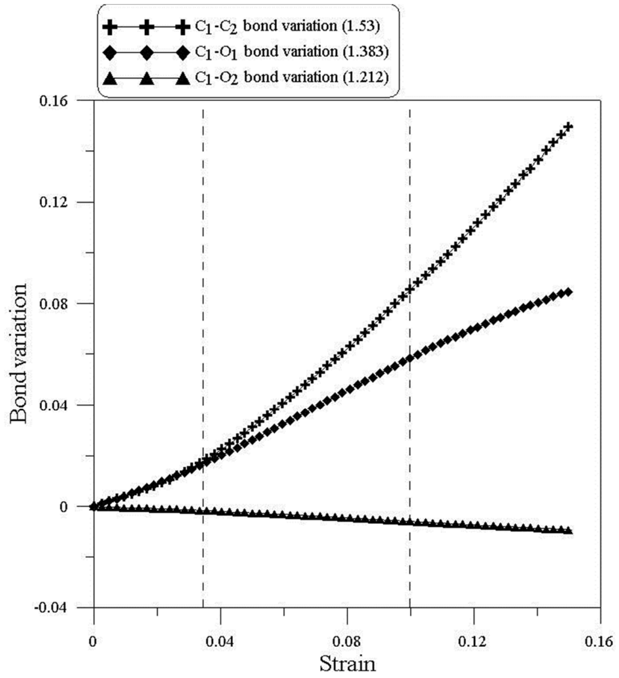

Fig. 3 The bond length variations of C_1-O_1, C_1-C_2, and C_1-O_2 pairs with strain.

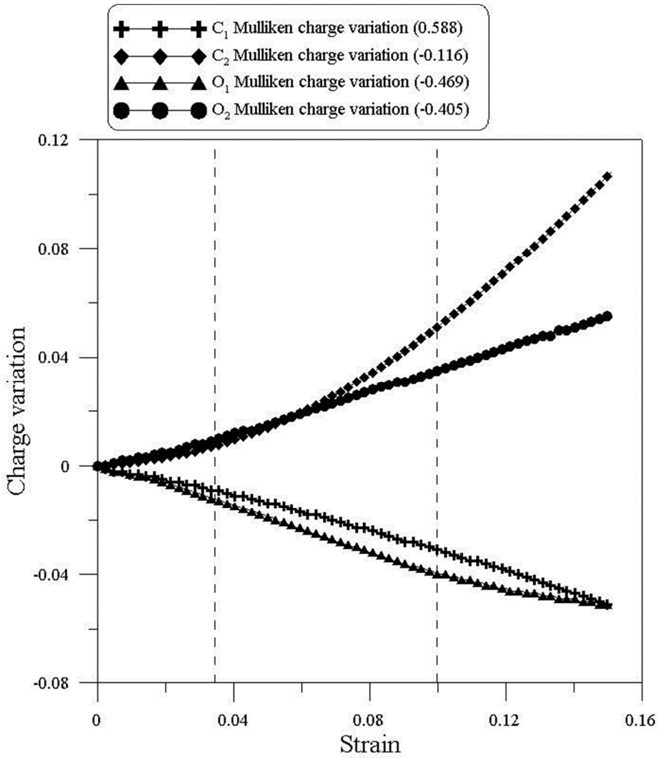

Fig. 4 The Mulliken charge variations of O_1, O_2, C_1, and C_2 atoms

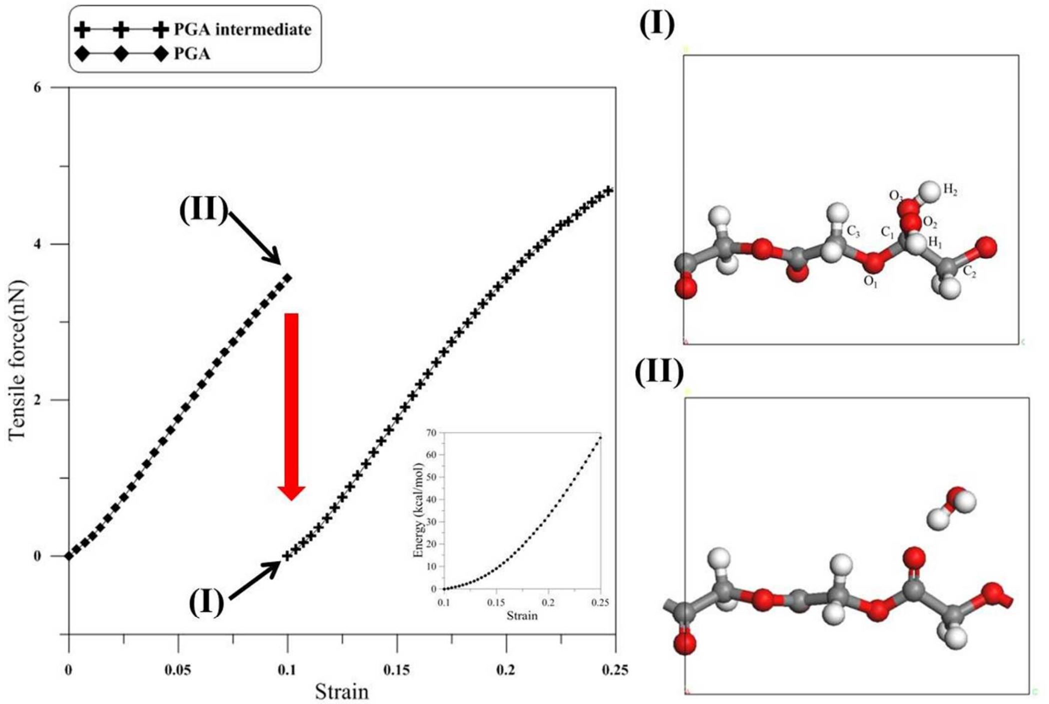

Fig. 5 The force-strain profile for the PGA hydrolysis intermediate at different strains. (bottom right panel) Structure from the combination of PGA and a water molecule; (upper right panel) PGA intermediate structure; and (inset) the variation of energy with strain for PGA intermediate.

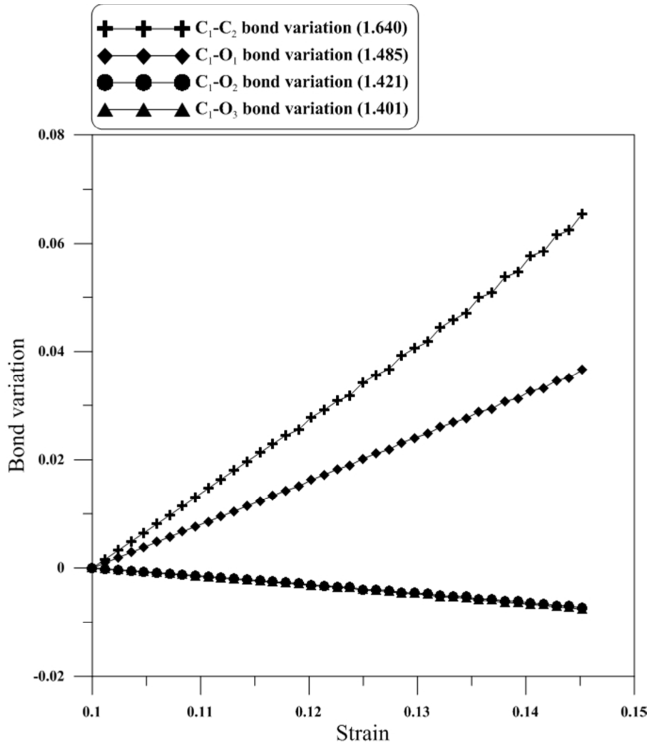

Fig. 6 Profiles of bond length variations with the strain for C_1-C_2, C_1-O_1, C_1-O_2, and C_1-O_3 bonds.

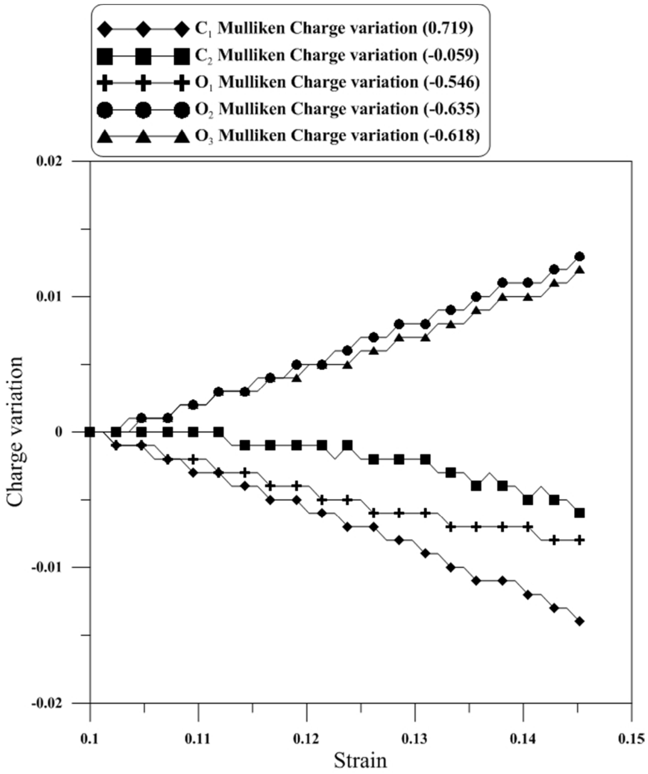

Fig. 7 Charge variations with strain for C_1, C_2, O_1, O_2, and O_3 atoms.

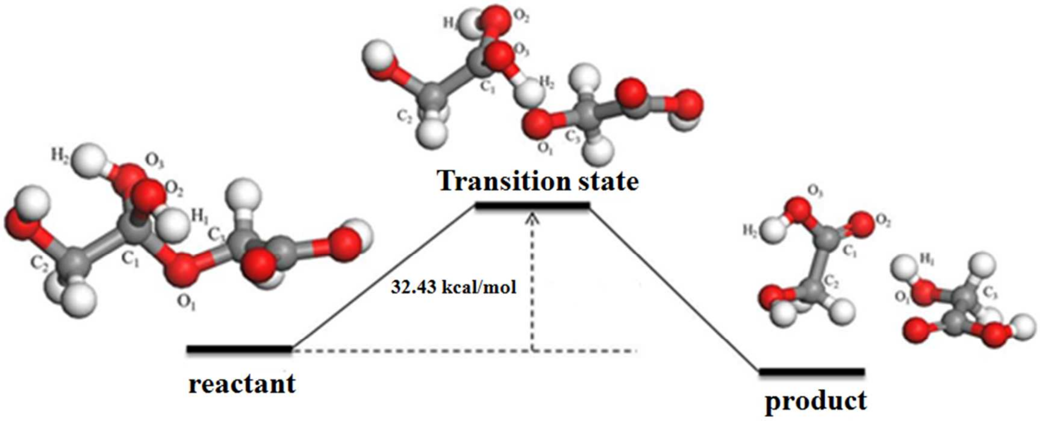

Fig. 8 Minimal energy pathway (MEP) for PGA intermediate degradation.

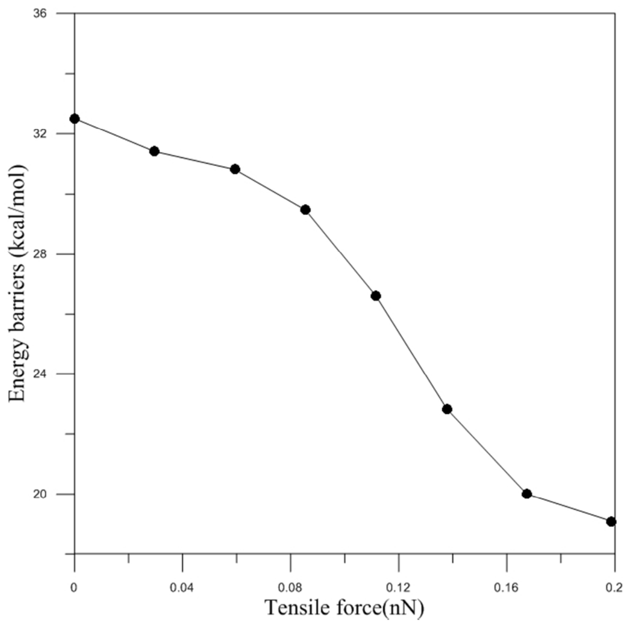

Fig. 9 Energy barriers at different tensile force for the PGA intermediate.